Research Article Vol. 6, No. 8 / August 2019 / Optica 1016

Dynamic suppression of Rayleigh backscattering in dielectric resonators

Seunghwi Kim,[1] Jacob M. Taylor,[2,3] and Gaurav Bahl[1,*]

[1]Mechanical Science and Engineering, University of Illinois at Urbana-Champaign, Urbana, Illinois 61801, USA
[2]Joint Quantum Institute, University of Maryland, College Park, Maryland 20742, USA
[3]National Institute of Standards and Technology, Gaithersburg, Maryland 20899, USA
*Corresponding author: bahl@illinois.edu

Received 7 February 2019; revised 27 June 2019; accepted 11 July 2019 (Doc. ID 359737); published 7 August 2019

The ultimate limits of performance for any classical optical system are set by sub-wavelength fluctuations within the host material, which may be frozen-in or even dynamically induced. The most common manifestation of such subwavelength disorder is Rayleigh light scattering, which is observed in nearly all waveguiding technologies today and can lead to both irreversible radiative losses as well as undesirable intermodal coupling. While it has been shown that backscattering from disorder can be suppressed by breaking the time-reversal symmetry in magneto-optic and topological insulator materials, common optical dielectrics possess neither of these properties. Here, we demonstrate an optomechanical approach for dynamically suppressing Rayleigh backscattering within dielectric resonators. We achieve this by locally breaking the time-reversal symmetry in a silica resonator through a Brillouin scattering interaction that is available in all materials. Near-complete suppression of Rayleigh backscattering is experimentally confirmed through two independent measurements—the elimination of a commonly seen normal-mode splitting or "doublet" effect and by measurement of the reduction in intrinsic optical loss. Additionally, a reduction of the back-reflections caused by disorder is also observed. Our results provide new evidence that it is possible to dynamically suppress Rayleigh backscattering within any optical dielectric medium using time-reversal symmetry breaking, for achieving robust light propagation in spite of scatterers or defects.

https://doi.org/10.1364/OPTICA.6.001016

1. INTRODUCTION

Rayleigh scattering is routinely encountered in nanostructured photonic devices [1,2], as it limits microresonator quality (Q) factors [3–5], affects the stability of frequency combs [6,7], causes Anderson localization [8], and limits the performance of metasurfaces [9]. It can be induced by inhomogeneities in the form of internal stresses, point defects, density variations, dislocations, and even surface roughness, which are unavoidable due to manufacturing limitations, but may also occur thermodynamically. In particular, back-reflections arising from Rayleigh scatterers in nanostructured devices create prominent reflections in silicon photonics [10] and a well-known mode splitting or "doublet" phenomenon in resonators [3–5,11], both of which impose severe technological constraints. While isolators and circulators can certainly block reflections, they are essentially dissipative in nature and only serve as a fix that does not suppress the original scattering event.

An elegant proposal to counteract disorder-induced backscattering of electromagnetic waves is to break the time-reversal symmetry (TRS) of the medium [12,13]—so that modes available for opposite, i.e., time-reversed, propagation are simply not symmetric in energy–momentum space. In other words, backscattering can be suppressed at the point of origin by establishing a large contrast in the optical density of states for propagation in the opposing directions. This effect has been experimentally confirmed in Faraday rotator (magneto-optic) materials biased with large magnetic fields [14] but cannot be extended to common dielectrics. A similar effect, in which broken TRS suppresses electron backscattering, is also seen in the chiral edge currents of two-dimensional electron systems exhibiting the quantum Hall effect (QHE) [15,16]. More recently, there has been a flurry of activity on backscattering suppression via TRS-breaking in photonic topological insulator metamaterials after the analogy to the QHE was established [17], with successful demonstration in a magneto-optic photonic crystal [18] and through Floquet pumping [19]. Unfortunately, since common photonic materials do not have magneto-optical activity and are topologically trivial insulators in their bandgaps, how these lessons may be mapped to any monolithic dielectric waveguide remains an open question.

In this work, we demonstrate a simple optomechanical approach by which we can dynamically suppress electromagnetic backscattering in any dielectric. The approach relies on a normal-mode splitting process supported by Brillouin light scattering, which is a high-gain optical nonlinearity available in all phases of matter, and has been established as a highly effective and generalizable tool for breaking TRS in dielectric waveguides and resonators [20–23]. The most convenient system in which

to demonstrate this principle is a high-Q microresonator, since these can tremendously lower the power threshold required for nonlinear optical processes, especially for Brillouin optomechanics [21,22,24]. We experimentally demonstrate near-complete suppression of Rayleigh backscattering within monolithic silica microresonators, with dynamic control provided by an external optical pump. The effect is confirmed through the elimination of the backscattering-induced normal-mode formation (or "doublet" mode) between degenerate cw and ccw modes of the symmetric resonator, as well as improved coupling to a waveguide due to the reduced optical loss. Our experiments exhibit a restoration to the intrinsic material loss rate of an optical resonator in spite of the presence of scattering defects.

2. PRINCIPLE

The system under consideration [Fig. 1(a)] is a symmetric whispering-gallery resonator (WGR) that supports two degenerate optical modes, $a_{\pm}$, associated with clockwise (+ or cw) and counterclockwise (– or ccw) photon propagation. Such degenerate modes, which are time-reversed partners, can be coupled through backscattering from inhomogeneities or defects, resulting in a well-known "doublet" mode if the coupling rate is comparable to the optical loss rate [3–5]. For lower backscattering rates, the mode only appears slightly broadened from its intrinsic line width. Figure 1(b) exhibits this backscattering-induced hybridization, measured in a silica microsphere WGR. The measurement is performed via evanescent probing through a tapered fiber waveguide [Fig. 1(a)] such that the optical resonances appear as a dip in transmission. Optical probing in both directions through the waveguide confirms that the $a_{\pm}$ modes are hybridized due to Rayleigh backscattering [3–5] and have lost their distinguishable directionality. It is this detrimental mode splitting and broadening effect that we wish to mitigate.

In order to experimentally shut down the effect of the backscattering channel between a_+ and a_-, we break time-reversal symmetry within the bandwidth of these modes. Specifically, we employ a Brillouin-scattering-induced normal-mode splitting process [21] that, due to intrinsic momentum conservation rules, allows us to only modify the susceptibility, $\chi_{a+}(\omega)$, of the a_+

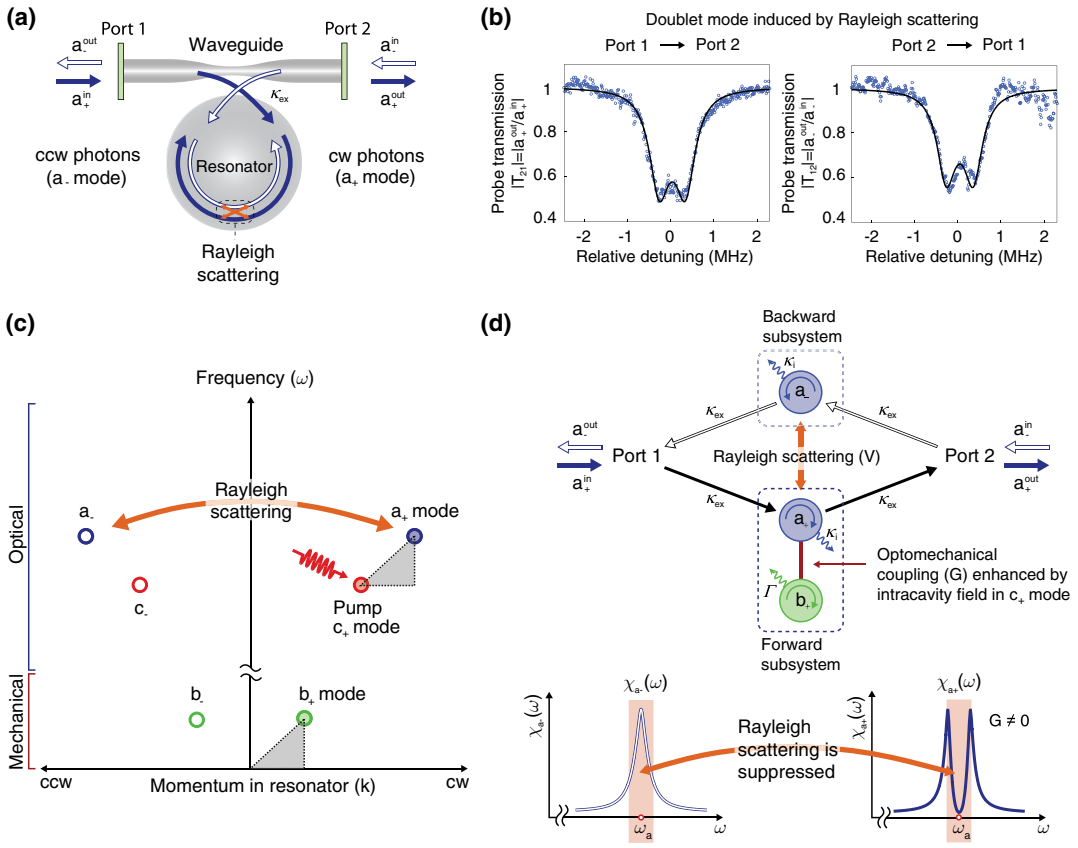

Fig. 1. Rayleigh backscattering in a whispering-gallery resonator (WGR) and concept for optomechanical suppression. (a) Optical WGRs support degenerate modes ($a_{\pm}$) that are time-reversed partners (cw/ccw) and can be individually accessed via directional probing. Rayleigh backscattering from disorder intrinsic to the WGR can couple these modes, leading to loss of their distinguishable directionality. (b) Experimentally, this results in normal-mode splitting or "doublet" (measured here in a silica WGR) when the disorder-induced backscattering rate is comparable to the intrinsic optical loss rate. Such doublets are routinely observed in high-Q resonator systems and impose a technological constraint. In this representative example, we observe a Rayleigh-backscattering-induced coupling rate of about $V = 0.33$ MHz. (c) We suppress Rayleigh backscattering by breaking time-reversal symmetry within the bandwidth of the $a_{\pm}$ optical modes. This is achieved through a Brillouin scattering process [21,25], in which a high-coherence cw mechanical mode, b_+, is coupled to the cw a_+ mode by a cw directional pump, c_+. The interaction is subject to the phase-matching constraint illustrated by the grey triangle. The momentum-matching requirement implies that the cw pump does not directly induce any effect for the ccw optical mode, a_-. (d) Toy model for the WGR and waveguide system, in which we distinguish the two directional subsystems and indicate both Rayleigh (V) and optomechanical (G) couplings. All variables are defined in the main text. The directional Brillouin optomechanical coupling significantly reduces the susceptibility of the a_+ mode only and "open-circuits" the backscattering channel, thereby suppressing Rayleigh scattering.

mode while leaving the a_- mode nominally unaffected [Fig. 1(d), bottom]. Similar to other optomechanically induced transparencies [26,27], the Brillouin-induced normal-mode splitting arises due to coherent coupling [28] between an optical mode with a long-lived propagating mechanical state that is enabled through radiation forces and photoelastic scattering. When the coupling rate between light and the mechanics is sufficiently large, the optical mode exhibits normal-mode splitting, which reduces the on-resonance optical density of states over a wide bandwidth and inhibits absorption from the waveguide. Production of the Brillouin normal-mode splitting requires a Stokes-detuned pump optical field (on a different optical mode, c_+) that co-propagates with the mode of interest, a_+, and a high-Q mechanical whispering-gallery mode, b_+, within the WGR. These three modes must together be subject to the Brillouin phase-matching condition on both frequency, $\omega_a = \omega_c + \omega_b$, and momentum, $k_a = k_c + k_b$, as illustrated in Fig. 1(c). In our experiment, we use c_+ pumping only, although a c_- pump could also be invoked to independently control the susceptibility for the a_- mode [25]. It is the unique, momentum-selective feature of this process that allows us to break TRS of the optical states within the resonator.

The model Hamiltonian for this system includes both Rayleigh backscattering and the Brillouin coupling as follows:

$$H_{\text{int}} = \hbar(G a_+^\dagger b_+ + G^* a_+ b_+^\dagger) + \hbar V(a_+^\dagger a_- + a_-^\dagger a_+). \quad (1)$$

Here, V is the Rayleigh-backscattering-induced coupling rate between the $a_\pm$ modes, while $G = g_o\sqrt{n_{c+}}$ is the pump-enhanced clockwise-only optomechanical coupling rate between the a_+ optical mode and the b_+ mechanical mode. g_o represents the single-photon optomechanical coupling rate, and n_{c+} represents the average number of intracavity photons in the c_+ mode. Since no ccw pump is applied to the system, an optomechanical interaction between a_- and b_- need not be considered. A detailed analysis presented in Section 1 of Supplement 1 additionally incorporates the effects of disorder-induced backscattering within the pump modes, $c_\pm$, which can be distinct from the Rayleigh coupling between $a_\pm$ due to differences of mode shape and polarization. However, as we show in Supplement 1, Sections 1.G–1.F, there is no evidence for this additional scattering effect within the pump modes, in the experiments that we discuss in this paper. In certain cases, the effective cw–ccw scattering rate also need not be symmetric [5,29,30]. However, this asymmetry is insignificant in cases where the scatterers are of deep subwavelength size and are randomly distributed, e.g., for intrinsic Rayleigh scattering occurring from material imperfections or surface roughness. In this study, we observed no evidence of asymmetric scattering, and a single scattering rate, V, is found to be adequate.

Figure 1(d) presents a toy model of the system, in which we explicitly distinguish between forward and backward subsystems. The degenerate optical modes, $a_\pm$, are modeled with intrinsic loss rate, κ_i, which includes all absorption and scattering mechanisms that leak light out of the mode, but excludes the influence of the backscattering channel, V. These modes, $a_\pm$, couple to the waveguide with an extrinsic coupling rate defined by κ_{ex} that is symmetric in both forward and backward directions. For light propagating in the waveguide from Port 1 → Port 2 (forward direction), the interaction with the resonator occurs through the forward subsystem described as the optomechanically coupled a_+ optical and b_+ mechanical modes. Conversely, for light propagating from Port 2 → Port 1 (backward direction), light primarily interacts with the a_- optical mode. Due to the different optical susceptibility of the forward and backward subsystems for any nonzero optomechanical coupling, the system exhibits broken time-reversal symmetry for transmission measurements. For reflections to take place in this system, i.e., Port 1 → Port 1, or Port 2 → Port 2, light must interact in series with both the forward and backward subsystems while passing through the Rayleigh backscattering channel (see illustration in Supplement 1, Fig. S1). Thus, the reflection coefficients measured at each port are necessarily identical.

We can analytically obtain the waveguide transmission coefficients (T_{21} in the forward direction, T_{12} in the backward direction) and reflection coefficients at each port ($R_{11} = R_{22} = R$) using the Heisenberg–Langevin equations for motion for this system in the rotating wave approximation (Supplement 1, Section 1). In any side-coupled resonator–waveguide system, the total optical loss rate, κ, is defined by both the extrinsic losses (from waveguide loading) and intrinsic losses through the expression $\kappa = \kappa_i + \kappa_{\text{ex}}$. The condition for "critical coupling"—defined as the point where on-resonance transmission reaches zero—can be derived as $\kappa = 2\kappa_{\text{ex}}$. Typically, this situation occurs when the intrinsic coupling rate, κ_{ex}, and the intrinsic loss rate, κ_i, are matched. However, in the case where both Rayleigh backscattering, V, and the optomechanical coupling, G, are acting on the modes [Fig. 1(d)], the optical loss rates for the $a_\pm$ modes are no longer identical, and the critical coupling conditions must also change. In the simplest case, in which all fields are on-resonance, the total effective loss rates for the $a_\pm$ modes can be evaluated as (details in Supplement 1, Section 1.B)

$$\kappa_{\text{eff}}^+ = \kappa(1 + \mathcal{C}) + \frac{4V^2}{\kappa}, \quad (2a)$$

$$\kappa_{\text{eff}}^- = \kappa + \frac{4V^2}{\kappa(1 + \mathcal{C})}. \quad (2b)$$

Here, we have introduced $\mathcal{C} = 4G^2/\kappa\Gamma$ as the optomechanical cooperativity, which is proportional to the intracavity photon number in the c_+ mode, n_{c+}. These expressions show that even if $\mathcal{C} = 0$, the Rayleigh backscattering introduces an additional intrinsic optical loss of $4V^2/\kappa$ to each mode, a loss channel formed through the counterpropagating mode. Moreover, we can see that as the optomechanical coupling rate is increased in the cw direction, light on-resonance in the ccw mode experiences a reduction in optical loss (κ_{eff}^- reduces) as an indirect effect. In the limit of large optomechanical coupling, $\mathcal{C} \to \infty$, the optical loss in the ccw mode approaches κ, i.e., the effective intrinsic loss, $\kappa_{\text{eff}}^- - \kappa_{\text{ex}}$, approaches the purely intrinsic loss rate, κ_i. In this case, the reflection should also approach zero since no backscattering occurs.

3. RESULTS

In order to test the predictions of the theoretical model, we perform a series of experiments using silica microsphere WGRs. Such resonators are easily produced by melting a tapered SMF-28e silica optical fiber through an arc discharge process, to result in a "ball-on-stick" geometry. In our first experiment with a 90 μm radius resonator, the Brillouin interaction is mediated by a mechanical whispering-gallery mode of frequency $\omega_b = 116.3$ MHz, having an azimuthal order of $M = 17$ around the resonator equator (corresponding to phonon wavenumber 0.030 μm^{-1}) and mechanical damping rate $\Gamma = (14.4 \pm 0.2)$ kHz. Experimental measurements of the optical doublet

resulting from Rayleigh backscattering in this device, without any optomechanical influence, were previously shown in Fig. 1(b). The pump (for controlling G) and probe (to observe $a_{\pm}$) are produced using a 1550 nm tunable external cavity diode laser and are evanescently coupled to the optical modes using a tapered fiber waveguide, as illustrated in Fig. 1(a). Further details on the experimental setup and calibration of the transmission and reflection coefficients are provided in Section 2 of Supplement 1. In Fig. 2, we present the measured transmission and reflection coefficients versus relative detuning, $\Delta = \omega_a - (\omega_{\text{pump}} + \omega_b)$, between the a_+ optical mode and the pump laser anti-Stokes mechanical sideband. A transparency window in the forward subsystem can be clearly observed as the relative detuning, Δ, approaches zero. Simultaneous measurements of the backward subsystem—the direction in which no pumping is performed—show that the a_- mode moves closer to critical coupling within the bandwidth of the nonreciprocal effect. At the same time, the reflection coefficient, $|R|$, measured from Port 1 shows a significant reduction on resonance due to the transparency-induced reduction of incoupling into mode a_+. However, as mentioned previously, this reflection coefficient is mathematically identical to the reflection measured at Port 2 [see also Eq. (S3c) and

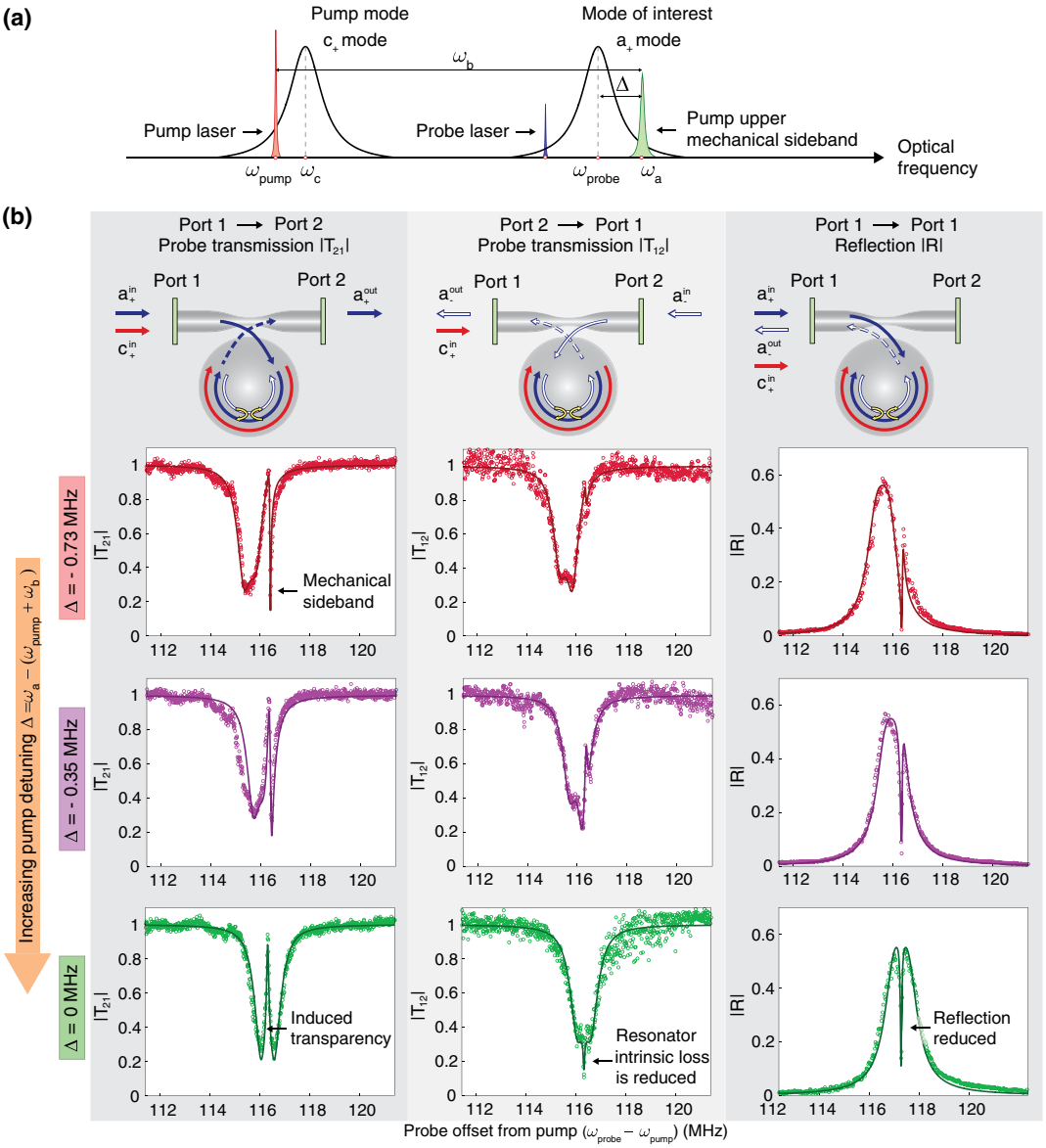

Fig. 2. Demonstration of dynamic optomechanical suppression of Rayleigh backscattering. (a) General configuration of optical pump, probe, and mechanical sidebands with respect to the c_+ and a_+ optical modes in the cw direction—used throughout this work. (b) This experiment uses a 116 MHz mechanical mode in a 90 μm radius silica WGR. The Rayleigh-scattering-induced doublet is readily observed in probing of the $a_{\pm}$ optical modes for an off-resonance pump. As the pump is brought on-resonance, the Brillouin-scattering-induced transparency is generated for the cw mode only (its on-resonance susceptibility is reduced), which breaks time-reversal symmetry within the bandwidth of the $a_{\pm}$ modes. These observations show two key predictions of the model—improved coupling of the a_- mode to the waveguide and the elimination of the doublet—both confirming the suppression of Rayleigh backscattering within the WGR. The reflection measurement at Port 1 represents a suppression of light coupling into the resonator due to the transparency. However, this Port 1 reflection should be identical to the reflection measured from Port 2 (Supplement 1, Section 1), which corresponds to a reduction in Rayleigh backscattering. Solid lines are simultaneous fits to the theoretical model. The reflection is very large due to resonant enhancement.

Fig. S1], which would actually correspond to a reduction in Rayleigh scattering from mode a_- into mode a_+. Unfortunately, we were unable to directly measure the Port 2 reflection coefficient since the large forward pump signal, c_+^{in}, at only 116 MHz offset makes this measurement technically very challenging. The detailed model presented in Supplement 1 allows extraction of the intrinsic optical loss rate [$\kappa_i = (0.35 \pm 0.03)$ MHz], the extrinsic optical loss rate {$\kappa_{\text{ex}} = (0.54 \pm 0.01)$ MHz [the optical mode is over-coupled]}, and the Rayleigh backscattering rate [$V = (0.34 \pm 0.01)$ MHz] for this experiment by simultaneously fitting all the measured traces. At resonance ($\Delta = 0$ MHz), we estimate $G = (0.17 \pm 0.01)$ MHz with an intracavity (pump) occupation number of $n_{c+} \simeq 1 \times 10^{10}$ and a single-photon optomechanical coupling rate, $g_o = (1.6 \pm 0.09)$ Hz. All uncertainties in this manuscript correspond to 95% confidence intervals of the fitted value.

To explore the limits of how strongly Rayleigh backscattering may be suppressed, we performed a second experiment on a 101 μm radius resonator (Fig. 3), mediated by a 229.5 MHz mechanical mode having azimuthal order $M = 39$ (corresponding to phonon wavenumber 0.062 μm^{-1}) and damping rate $\Gamma = (39.1 \pm 1.3)$ kHz. Here, we use a higher optical pump power to bring the system into the Brillouin strong-coupling regime [25,28], where the optomechanical coupling exceeds the total optical loss rate ($G \geq \kappa/2$). We first detune the pump sufficiently so that the optomechanical coupling is negligible [$G = 0$, Fig. 3(a)]. The $a_\pm$ modes exhibit the doublet characteristic, as expected from Rayleigh backscattering within the resonator. Fitting to the theoretical model allows us to discern the backscattering strength at $V = (0.3 \pm 0.01)$ MHz, intrinsic loss $\kappa_i = (0.45 \pm 0.02)$ MHz, and extrinsic coupling for the experiment at $\kappa_{\text{ex}} = (0.17 \pm 0.003)$ MHz, all of which contribute to the measured line shape. Strong optomechanical coupling occurs when the laser is near zero detuning and manifests as an avoided crossing in both optical and mechanical spectra as a function of pump detuning. This is confirmed by experimental measurements for a forward-directed pump and probe in Fig. 3(c). Mechanical spectra are measured using the beating between the pump and the forward scattered light on a photodetector [31]. The experimental observation of the avoided crossing closely matches the theoretically modeled eigenfrequencies [$\lambda_\pm$ in Fig. 3(c), right]. A detailed discussion on this observation is provided in Section 1.F of Supplement 1.

We now bring the cw pump laser exactly on resonance ($\Delta = 0$ MHz) such that 272 μW optical power is absorbed into

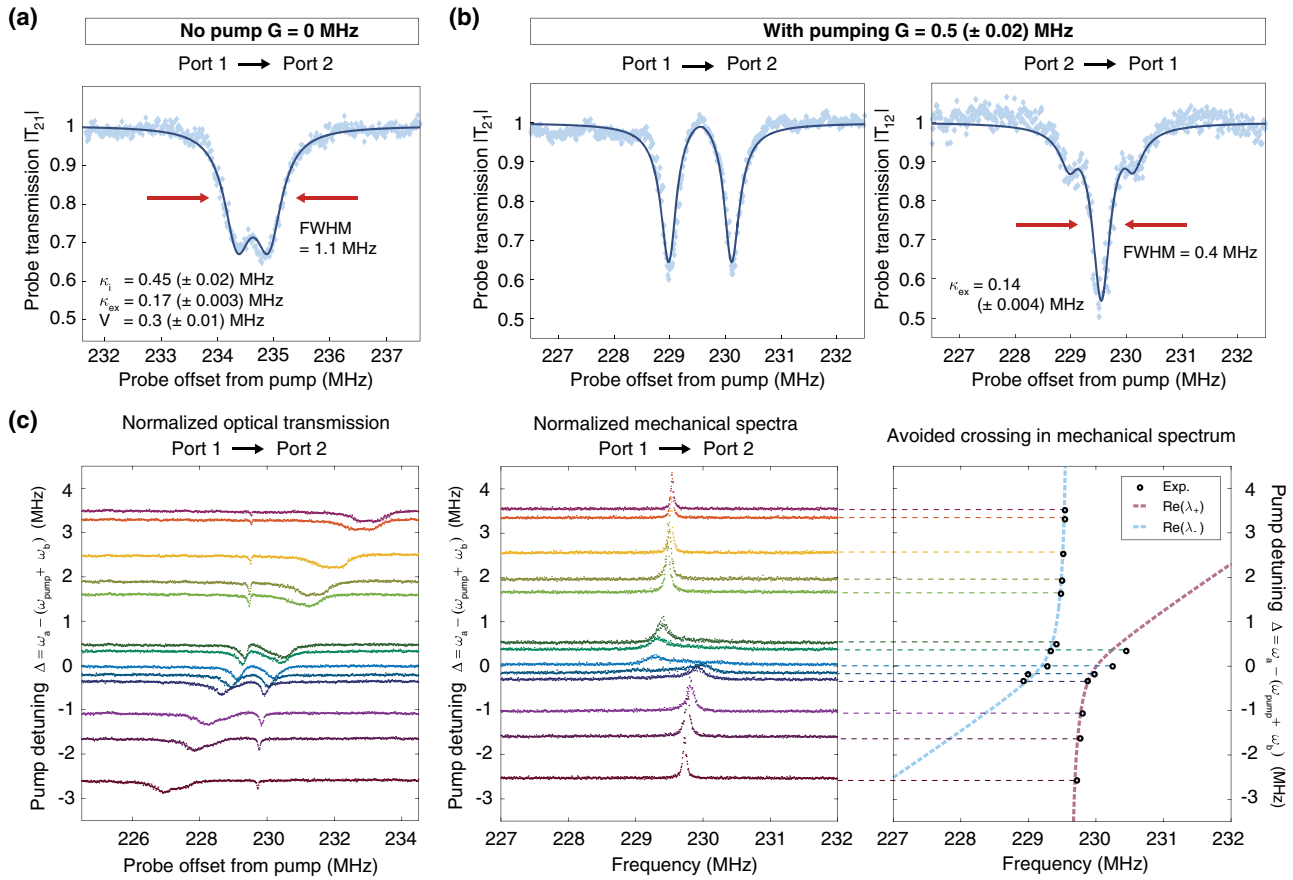

Fig. 3. Near-complete suppression of Rayleigh backscattering with Brillouin strong coupling. (a) This experiment was performed with the 229.5 MHz mechanical mode of a 101 μm radius silica WGR. By initially detuning the pump laser we observe the Rayleigh-backscattering-induced optical doublet. Fitting to the theoretical model (solid line) indicates intrinsic loss, κ_i, extrinsic loss, κ_{ex}, and backscattering rate, V. (b) We now set the pump to zero detuning so that strong cw optomechanical coupling is achieved (with $G = 0.5$ MHz), resulting in a prominent change in susceptibility for the cw (a_+) mode only. The time-reversed (a_-) mode, which we did not modify, simultaneously exhibits much narrower line width, and the backscattering-induced doublet is eliminated. (c) The avoided crossing due to Brillouin strong coupling is observed in both the optical transmission spectrum and the mechanical spectrum for various detunings of the pump. The data closely match the theoretical eigenfrequencies (see Section 1.F of Supplement 1). Mechanical spectra are measured from the beating between the pump and scattered light on a photodetector [31].

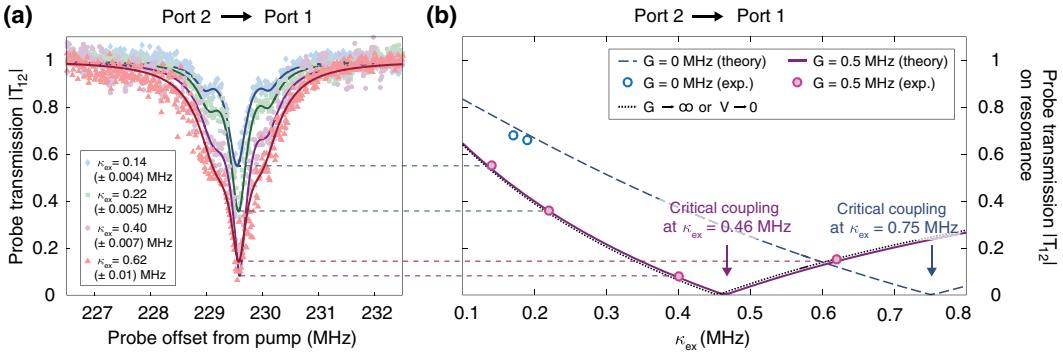

Fig. 4. Determination of intrinsic loss rate and suppression of Rayleigh-backscattering-induced loss. (a) By adjusting the extrinsic coupling between the resonator and waveguide, κ_{ex}, we are able to explore the point of critical coupling for the ccw mode, a_-. Critical coupling is the point where on-resonance transmission reaches zero and occurs when the extrinsic coupling rate, κ_{ex}, and the intrinsic loss rate, κ_i, are matched. (b) We use experimentally measured parameters in the theoretical model [Supplement 1, Eq. (S8)] to establish theoretical predictions for the on-resonance transmission as a function of extrinsic coupling rate. When optomechanical coupling is zero (i.e., Rayleigh backscattering is active) the predicted critical coupling point is at 0.75 MHz. Experimental data points (blue) are well matched to this predicted curve. On the other hand, with an optomechanical coupling of $G = 0.5$ MHz, we estimate a ccw effective intrinsic loss rate of 0.46 MHz, a very close match to the purely intrinsic loss rate of 0.45 MHz. The measured on-resonance transmission (red) from the experimental measurements in (a) are also very well matched to the theoretical predictions from the model. We additionally plot the theoretical case where Rayleigh scattering does not contribute (occurs when either $V \to 0$ or $G \to \infty$).

the resonator, leading to an estimated optomechanical coupling rate of $G = (0.5 \pm 0.02)$ MHz. The resulting Brillouin-induced normal-mode splitting in the a_+ mode can be observed through forward transmission measurement [Fig. 3(b), left]. Since the TRS broken bandwidth now encompasses nearly the whole of the counterpropagating a_- mode, the backscattering will be significantly suppressed. Simultaneous measurement of backward transmission [Fig. 3(b), right] reveals that the Rayleigh-backscattering-induced doublet indeed does disappear when measuring the a_- mode, and there is a significant improvement in the resonance line width. Furthermore, the on-resonance optical transmission in this direction dips lower, as evidence of reduced optical losses within the resonator. Next, we quantitatively verify this reduction in resonator loss.

As discussed above in Eq. (2b) (see also Supplement 1, Fig. S3), in the limit of large optomechanical coupling, the Rayleigh backscattering can be mitigated completely, and the effective intrinsic loss of the ccw a_- mode must converge to its purely intrinsic loss rate, $\kappa_i = 0.45$ MHz. This is experimentally verifiable, provided that we observe critical coupling in the waveguide–resonator system when extrinsic coupling $\kappa_{ex} \approx 0.45$ MHz. In fact, measurement of the critical coupling point through a sweep of κ_{ex} is the only directly accessible measurement of the on-resonance intrinsic optical loss since the optical mode shape is non-Lorentzian. First, we use the loss rates and coupling rates extracted earlier to establish that critical coupling for $G = 0$ will occur when $\kappa_{ex} = 0.75$ MHz due to the increased intrinsic loss $(+4V^2/\kappa)$ from the Rayleigh backscattering channel. Experimental data points for zero optomechanical coupling match well to this theoretical prediction [see Fig. 4(b)]. Then, we experimentally test the case when $G = 0.5$ MHz by sweeping κ_{ex} from 0.14 to 0.62 MHz. Here, κ_{ex} is increased by moving the tapered fiber close to the resonator [32]. Note that the Rayleigh contribution to the ccw effective intrinsic loss $(4V^2/\kappa(1 + C))$ also reduces with increasing κ_{ex}. Measurements of the ccw mode in Figs. 4(a) and 4(b) show the evolution of the ccw resonance, as it proceeds from undercoupling to overcoupling while passing through the critical coupling point. The theoretical model and experimental data both indicate that critical coupling must occur at $\kappa_{ex} \approx 0.46$ MHz. This is extremely close to the estimated purely intrinsic loss rate of $\kappa_i = (0.45 \pm 0.02)$ MHz and is well within the error bars. This indicates that the TRS-broken system achieves nearly complete suppression of the undesirable Rayleigh backscattering in the limit of large G. As predicted by the theoretical model (Supplement 1, Section 1.D), an even higher optomechanical coupling rate could enable recovery of the Lorentzian line shape of the ccw optical mode.

4. DISCUSSION

Our experiments demonstrate the fundamental concept that local time-reversal symmetry-breaking interactions can suppress Rayleigh backscattering from disorder within dielectrics. While we have used a specific narrowband optomechanical approach in this work, the principle can readily be translated to other TRS-breaking techniques encompassing nonlinear optics [20,33,34], chirally pumped atoms [35], parity-time symmetry breaking [36,37], spatiotemporal modulation [38], electro-optic interaction [39], and even magneto-optic nonlinearity [40]. We anticipate applications of this principle for fiber networks and integrated waveguides, where broadband TRS-breaking has already been demonstrated via nonmagnetic and Brillouin approaches [23,38,41], but suppression of disorder-induced backscattering has not.

Funding. National Science Foundation (NSF) (EFMA-1627184); Air Force Office of Scientific Research (AFOSR) (FA9550-15-1-0234); Office of Naval Research (ONR) (N00014-17-1-2209); National Institute of Standards and Technology (NIST).

See Supplement 1 for supporting content.

REFERENCES

1. D. Marcuse, "Mode conversion caused by surface imperfections of a dielectric slab waveguide," Bell Syst. Tech. J **48**, 3187–3215 (1969).
2. D. Pinnow, T. Rich, F. Ostermayer, and M. DiDomenico, "Fundamental optical attenuation limits in the liquid and glassy state with application

to fiber optical waveguide materials," App. Phys. Lett. **22**, 527–529 (1973).
3. D. S. Weiss, V. Sandoghdar, J. Hare, V. Lefèvre-Seguin, J.-M. Raimond, and S. Haroche, "Splitting of high-Q Mie modes induced by light backscattering in silica microspheres," Opt. Lett. **20**, 1835–1837 (1995).
4. M. L. Gorodetsky, A. D. Pryamikov, and V. S. Ilchenko, "Rayleigh scattering in high-Q microspheres," J. Opt. Soc. Am. B **17**, 1051–1057 (2000).
5. A. Mazzei, S. Götzinger, L. de S. Menezes, G. Zumofen, O. Benson, and V. Sandoghdar, "Controlled coupling of counterpropagating whispering-gallery modes by a single Rayleigh scatterer: a classical problem in a quantum optical light," Phys. Rev. Lett. **99**, 173603 (2007).
6. A. G. Griffith, R. K. W. Lau, J. Cardenas, Y. Okawachi, A. Mohanty, R. Fain, Y. H. D. Lee, M. Yu, C. T. Phare, C. B. Poitras, A. L. Gaeta, and M. Lipson, "Silicon-chip mid-infrared frequency comb generation," Nat. Commun. **6**, 6299 (2015).
7. M.-G. Suh, Q.-F. Yang, K. Y. Yang, X. Yi, and K. J. Vahala, "Microresonator soliton dual-comb spectroscopy," Science **354**, 600–603 (2016).
8. T. Schwartz, G. Bartal, S. Fishman, and M. Segev, "Transport and Anderson localization in disordered two-dimensional photonic lattices," Nature **446**, 52–55 (2007).
9. P. Nagpal, N. C. Lindquist, S.-H. Oh, and D. J. Norris, "Ultrasmooth patterned metals for plasmonics and metamaterials," Science **325**, 594–597 (2009).
10. F. Morichetti, A. Canciamilla, C. Ferrari, M. Torregiani, A. Melloni, and M. Martinelli, "Roughness induced backscattering in optical silicon waveguides," Phys. Rev. Lett. **104**, 033902 (2010).
11. T. J. Kippenberg, A. L. Tchebotareva, J. Kalkman, A. Polman, and K. J. Vahala, "Purcell-factor-enhanced scattering from Si nanocrystals in an optical microcavity," Phys. Rev. Lett. **103**, 027406 (2009).
12. A. A. Golubentsev, "The suppression of interference effects in multiple scattering of light," Sov. Phys. JETP **59**, 26–32 (1984).
13. F. C. MacKintosh and S. John, "Coherent backscattering of light in the presence of time-reversal-noninvariant and parity-nonconserving media," Phys. Rev. B **37**, 1884–1897 (1988).
14. R. Lenke and G. Maret, "Magnetic field effects on coherent backscattering of light," Eur. Phys. J. B **17**, 171–185 (2000).
15. B. I. Halperin, "Quantized hall conductance, current-carrying edge states, and the existence of extended states in a two-dimensional disordered potential," Phys. Rev. B **25**, 2185–2190 (1982).
16. M. Büttiker, "Absence of backscattering in the quantum hall effect in multiprobe conductors," Phys. Rev. B **38**, 9375–9389 (1988).
17. F. D. M. Haldane and S. Raghu, "Possible realization of directional optical waveguides in photonic crystals with broken time-reversal symmetry," Phys. Rev. Lett. **100**, 013904 (2008).
18. Z. Wang, Y. Chong, J. D. Joannopoulos, and M. Soljacic, "Observation of unidirectional backscattering-immune topological electromagnetic states," Nature **461**, 772–775 (2009).
19. M. C. Rechtsman, J. M. Zeuner, Y. Plotnik, Y. Lumer, D. Podolsky, F. Dreisow, S. Nolte, M. Segev, and A. Szameit, "Photonic Floquet topological insulators," Nature **496**, 196–200 (2013).
20. M. S. Kang, A. Butsch, and P. St. J. Russell, "Reconfigurable light-driven opto-acoustic isolators in photonic crystal fibre," Nat. Photonics **5**, 549–553 (2011).
21. J. Kim, M. C. Kuzyk, K. Han, H. Wang, and G. Bahl, "Non-reciprocal Brillouin scattering induced transparency," Nat. Phys. **11**, 275–280 (2015).
22. S. Kim, X. Xu, J. M. Taylor, and G. Bahl, "Dynamically induced robust phonon transport and chiral cooling in an optomechanical system," Nat. Commun. **8**, 205 (2017).
23. E. A. Kittlaus, N. T. Otterstrom, P. Kharel, S. Gertler, and P. T. Rakich, "Non-reciprocal interband Brillouin modulation," Nat. Photonics **12**, 613–619 (2018).
24. G. Bahl, M. Tomes, F. Marquardt, and T. Carmon, "Observation of spontaneous Brillouin cooling," Nat. Phys. **8**, 203–207 (2012).
25. J. Kim, S. Kim, and G. Bahl, "Complete linear optical isolation at the microscale with ultralow loss," Sci. Rep. **7**, 1647 (2017).
26. S. Weis, R. Rivière, S. Deléglise, E. Gavartin, O. Arcizet, A. Schliesser, and T. J. Kippenberg, "Optomechanically induced transparency," Science **330**, 1520–1523 (2010).
27. A. H. Safavi-Naeini, T. P. M. Alegre, J. Chan, M. Eichenfield, M. Winger, Q. Lin, J. T. Hill, D. E. Chang, and O. Painter, "Electromagnetically induced transparency and slow light with optomechanics," Nature **472**, 69–73 (2011).
28. S. Groblacher, K. Hammerer, M. R. Vanner, and M. Aspelmeyer, "Observation of strong coupling between a micromechanical resonator and an optical cavity field," Nature **460**, 724–727 (2009).
29. B. Peng, Ş. K. Özdemir, M. Liertzer, W. Chen, J. Kramer, H. Yılmaz, J. Wiersig, S. Rotter, and L. Yang, "Chiral modes and directional lasing at exceptional points," Proc. Natl. Acad. Sci. U.S.A. **113**, 6845–6850 (2016).
30. Q. Li, A. A. Eftekhar, Z. Xia, and A. Adibi, "Unified approach to mode splitting and scattering loss in high-Q whispering-gallery-mode microresonators," Phys. Rev. A **88**, 033816 (2013).
31. S. Kim and G. Bahl, "Role of optical density of states in Brillouin optomechanical cooling," Opt. Express **25**, 776–784 (2017).
32. M. Cai, O. Painter, and K. J. Vahala, "Observation of critical coupling in a fiber taper to a silica-microsphere whispering-gallery mode system," Phys. Rev. Lett. **85**, 74–77 (2000).
33. Z. Shen, Y.-L. Zhang, Y. Chen, C.-L. Zou, Y.-F. Xiao, X.-B. Zou, F.-W. Sun, G.-C. Guo, and C.-H. Dong, "Experimental realization of optomechanically induced non-reciprocity," Nat. Photonics **10**, 657–661 (2016).
34. L. D. Bino, J. M. Silver, M. T. M. Woodley, S. L. Stebbings, X. Zhao, and P. Del'Haye, "Microresonator isolators and circulators based on the intrinsic nonreciprocity of the Kerr effect," Optica **5**, 279–282 (2018).
35. C. Sayrin, C. Junge, R. Mitsch, B. Albrecht, D. O'Shea, P. Schneeweiss, J. Volz, and A. Rauschenbeutel, "Nanophotonic optical isolator controlled by the internal state of cold atoms," Phys. Rev. X **5**, 041036 (2015).
36. C. E. Rüter, K. G. Makris, R. El-Ganainy, D. N. Christodoulides, M. Segev, and D. Kip, "Observation of parity-time symmetry in optics," Nat. Phys. **6**, 192–195 (2010).
37. B. Peng, S. K. Özdemir, F. Lei, F. Monifi, M. Gianfreda, G. L. Long, S. Fan, F. Nori, C. M. Bender, and L. Yang, "Parity-time-symmetric whispering-gallery microcavities," Nat. Phys. **10**, 394–398 (2014).
38. H. Lira, Z. Yu, S. Fan, and M. Lipson, "Electrically driven nonreciprocity induced by interband photonic transition on a silicon chip," Phys. Rev. Lett. **109**, 033901 (2012).
39. A. Rueda, F. Sedlmeir, M. C. Collodo, U. Vogl, B. Stiller, G. Schunk, D. V. Strekalov, C. Marquardt, J. M. Fink, O. Painter, G. Leuchs, and H. G. L. Schwefel, "Efficient microwave to optical photon conversion: an electro-optical realization," Optica **3**, 597–604 (2016).
40. L. Bi, J. Hu, P. Jiang, D. H. Kim, G. F. Dionne, L. C. Kimerling, and C. A. Ross, "On-chip optical isolation in monolithically integrated non-reciprocal optical resonators," Nat. Photonics **5**, 758–762 (2011).
41. I. K. Hwang, S. H. Yun, and B. Y. Kim, "All-fiber-optic nonreciprocal modulator," Opt. Lett. **22**, 507–509 (1997).